Evidence of multiple reconnection lines at the magnetopause from cusp observations

K. J. Trattner,[1] S. M. Petrinec,[1] S. A. Fuselier,[1] N. Omidi,[2] and D. G. Sibeck[3]

Received 16 August 2011; revised 18 November 2011; accepted 22 November 2011; published 25 January 2012.

[1] Recent global hybrid simulations investigated the formation of flux transfer events (FTEs) and their convection and interaction with the cusp. Based on these simulations, we have analyzed several Polar cusp crossings in the Northern Hemisphere to search for the signature of such FTEs in the energy distribution of downward precipitating ions: precipitating ion beams at different energies parallel to the ambient magnetic field and overlapping in time. Overlapping ion distributions in the cusp are usually attributed to a combination of variable ion acceleration during the magnetopause crossing together with the time-of-flight effect from the entry point to the observing satellite. Most "step up" ion cusp structures (steps in the ion energy dispersions) only overlap for the populations with large pitch angles and not for the parallel streaming populations. Such cusp structures are the signatures predicted by the pulsed reconnection model, where the reconnection rate at the magnetopause decreased to zero, physically separating convecting flux tubes and their parallel streaming ions. However, several Polar cusp events discussed in this study also show an energy overlap for parallel-streaming precipitating ions. This condition might be caused by reopening an already reconnected field line, forming a magnetic island (flux rope) at the magnetopause similar to that reported in global MHD and Hybrid simulations.

Citation: Trattner, K. J., S. M. Petrinec, S. A. Fuselier, N. Omidi, and D. G. Sibeck (2012), Evidence of multiple reconnection lines at the magnetopause from cusp observations, *J. Geophys. Res.*, *117*, A01213, doi:10.1029/2011JA017080.

1. Introduction

[2] One manifestation of time-dependent reconnection at the magnetopause is a phenomenon known as a flux transfer event (FTE) [*Russell and Elphic*, 1979]. FTE's near the low-latitude magnetopause exhibit a bipolar magnetic field signature of the component normal to the magnetopause. This signature was interpreted as the motion of an open flux tube produced by transient magnetic reconnection [*Russell and Elphic*, 1978]. Plasma and energetic particle observations [e.g., *Berchem and Russell*, 1984; *Rijnbeek et al.*, 1984; *Farrugia et al.*, 1988; *Le et al.*, 1999], multispacecraft observations [*Elphic and Southwood*, 1987; *Wild et al.*, 2005, *Dunlop et al.*, 2005] and conjunctions of satellite and radar observations [*Lockwood et al.*, 2001; *Wild et al.*, 2001] have all supported the association of the bipolar FTE signature with time-dependent magnetic reconnection.

[3] Despite decades of research, there are many open questions concerning to the nature and occurrence of FTE's. While *Lockwood and Wild* [1993] suggested that FTE's are driven by variations in the Interplanetary Magnetic Field (IMF) in which the B_Z component becomes more southward, no such correlation with the southward turning of the IMF was reported by *Le et al.* [1993]. *Russell et al.* [1996] went even further by reporting no evidence for a connection between outside drivers and the occurrence rate of FTE's.

[4] The periodicity of FTE's was reported to be on average about 8 min [*Rijnbeek et al.*, 1984, *Russell et al.*, 1996]. A similar result was reported by *Lockwood and Wild* [1993] where they found that the time between successive FTE's varies from 1.5 to 18.5 min with an average of 8 min and a most common value of 3 min. This wide spectrum is similar to the distribution of IMF B_Z variations.

[5] In general, however, the FTE formation mechanism remains elusive. Several models invoke time-varying reconnection at the magnetopause with X line(s) at different locations and/or spatial extents to explain the nature of FTE's. The original patchy reconnection model (reconnection that varies both in time and in location at the magnetopause) [*Russell and Elphic*, 1978] predicts a pair of elbow shaped flux ropes of reconnected field lines generated by intermittent and localized reconnection which cross the magnetopause through approximately circular flux tubes that extend outward into the solar wind. The characteristic bipolar signature is caused by draping of surrounding magnetic fields around these flux tubes. This model is supported by a statistical analysis of 634 FTEs from the ISEE mission [*Kawano and Russell*, 2005], which showed a shorter longitudinal scale of the flux ropes compared to their latitudinal scale.

[1]Advanced Technology Center, Lockheed Martin Space Systems Company, Palo Alto, California, USA.
[2]Solana Scientific Inc., Solana Beach, California, USA.
[3]NASA Goddard Space Flight Center, Greenbelt, Maryland, USA.

0148-0227/12/2011JA017080

[6] *Scholer* [1988] suggested a model based on bursty reconnection along a single extended reconnection line (X line). In their model an enhancement and subsequent reduction of the reconnection rate at an X line generates bubble-like structures at the magnetopause which propagate along the magnetopause and produce the observed bipolar signature. Such a traveling bulge was observed by *Lockwood and Hapgood* [1998] for an FTE observed by AMPTE.

[7] A model based on multiple X lines was introduced by *Lee and Fu* [1985]. Already reconnected magnetic field lines at the magnetopause re-reconnect while the field line is convecting [e.g., *Zong et al.*, 2005; *Hasegawa et al.*, 2006; *Zhang et al.*, 2008; *Boudouridis et al.*, 2001]. Such a scenario forms magnetic loops or islands at the magnetopause as often depicted in 2-D representations. The observation of flow reversals in the boundary layer has been interpreted as evidence for the existence of multiple reconnection lines at the magnetopause [e.g., *Hasegawa et al.*, 2010].

[8] Evidence of re-reconnection at the magnetopause has also been discussed in cusp observations [e.g., *Fuselier et al.*, 1997]. Every reconnection process occurring at the magnetopause will leave a signature in the precipitating ion distribution in the cusps. The cusp signature of multiple reconnection lines is overlapping precipitating ion beams at different energies.

[9] *Yamauchi and Lundin* [1994] showed overlapping upward steps in energy superposed on the typical cusp downward ramp of an energy-latitude dispersion. These upward and downward steps were interpreted as evidence for multiple access of magnetosheath plasma to the same flux tube at different times. However, *Lockwood* [1995] pointed out that these observations could be also interpreted as a single pulsed reconnection together with finite gyroradius effects. The overlap in the data occurred only for non-field-aligned ions, due to their finite gyroradii. Downward precipitating field-aligned ions showed only an upward step and no overlap. According to *Lockwood* [1995] this upward step is caused by a reconnection rate which goes to zero between two pulses and switches off field-aligned ions, while higher–pitch angle ions are still seen due to their different times of flight.

[10] Overlapping cusp ion beams are also described in a model by *Lockwood* [1995] based on continuous particle entry along a newly opened field line. The overlap is caused by the variation in ion acceleration on crossing the magnetopause combined with the ion time-of-flight effect from the entry point to the observing satellite. Variations in ion acceleration could be caused by changes in solar wind velocity or a reconnection location in the opposing hemisphere to the observing satellite. In this scenario, a newly opened magnetic field line first has to progress against the magnetosheath flow until it reaches the equator. From there it convects with the magnetosheath flow.

[11] In a study by *Trattner et al.* [1998], overlapping ion observations did not satisfy all of the above described conditions. Observations showed a multitude of overlapping precipitating ion energy traces at lower and higher energies while the original trace was unaffected by these onsets, indicating that steady reconnection conditions occurred at the original X line location in conjunction with temporal reconnection events at secondary locations. Traces were well separated in energy and also overlapped for field-aligned ions, in contrast to observations reported by *Yamauchi and Lundin* [1994]. In addition, overlapping traces did not bifurcate from preexisting cusp dispersion and also did not merge at higher latitudes as described in the model by *Lockwood* [1995]. Instead, they disappeared within seconds, leaving the original trace unaffected. Solar wind conditions for observed overlaps were stable, which also does not satisfy conditions of a rapid change in the Alfvén velocity as described in the *Lockwood* [1995] model.

[12] Reopening of an existing flux tube and the formation of magnetic islands or plasmoids were also discussed in recent Hybrid simulations by *Omidi and Sibeck* [2007]. These magnetic islands are convected toward the cusp region where they are destroyed through secondary reconnection with lobe field lines. In this study we use three Polar cusp crossings and their specific solar wind and IMF conditions to investigate similarities for the occurrence of overlapping cusp ion dispersions. All discussed events occurred around the equinoxes and showed the typical overlapping cusp signatures for formation of a second reconnection line.

2. Instrumentation and Methodology

[13] The three events analyzed in this study are selected from a much larger Northern Hemisphere cusp survey containing about 1500 Polar cusp crossings. Ion distributions were obtained by the Toroidal Imaging Mass-Angle Spectrograph (TIMAS) [*Shelley et al.*, 1995] on board the Polar spacecraft.

[14] Polar/TIMAS proton measurements cover the energy range from 15 eV/e to 33 keV/e in 28 energy steps and provide 98% coverage of the unit sphere during a 6 s spin period. The Polar spacecraft was launched on 24 February 1996 into a nearly 90° inclination orbit with a perigee of about 2 R_E and an apogee of about 9 R_E. Polar crosses the cusp regions during two periods each year, with each period lasting several months. Cusp ion distributions are observed at altitudes between 3.5 and 9 R_E and up to 90° invariant latitude (ILAT).

[15] In addition to Polar ion data, solar wind context measurements observed by the Wind Magnetic Field Instrument (MFI) [*Lepping et al.*, 1995] and the Wind Solar Wind Experiment (SWE) [*Ogilvie et al.*, 1995] are used. These data are provided by the ISTP key parameter web page. Solar wind observations are convected to the magnetopause.

[16] Measurements of TIMAS 3-D plasma distributions are used to estimate the distance to the reconnection site and determine its location in order to establish if the reconnection site is in the same hemisphere as the observing satellite. The location of the reconnection line with respect to the observing satellite is one of the causes for the appearance of overlapping precipitating ion beams [*Lockwood*, 1995]. The procedure used for this distance estimate is generally known as the low-velocity cutoff method and is based on time-of-flight characteristics of precipitating ions in the cusp as first used by *Onsager et al.* [1990, 1991] in the Earth's plasma sheet boundary layer. Low-velocity cutoffs from precipitating and mirrored ion distributions in the cusp together with the known distance between the observing satellite and the

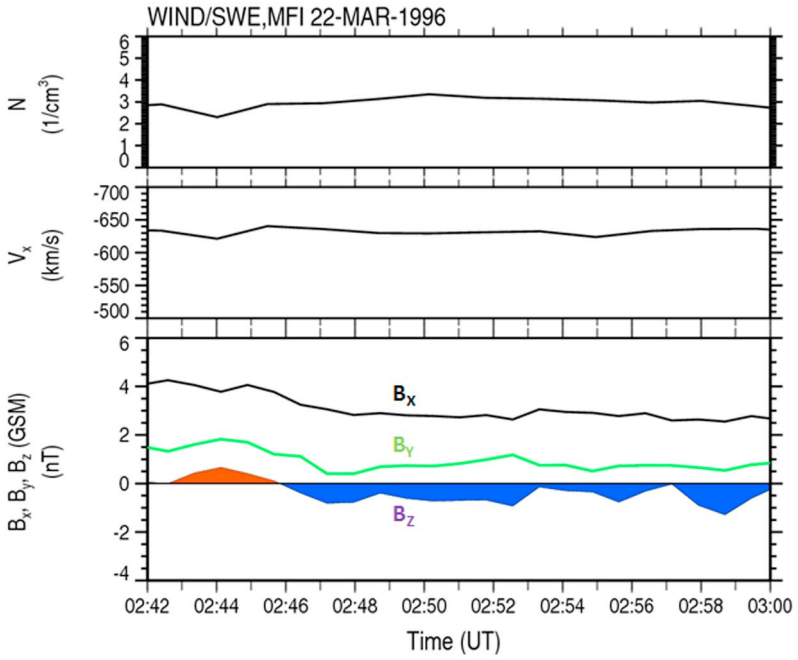

Figure 1. The solar wind and interplanetary magnetic field conditions during the 22 March 1996 Polar/TIMAS cusp crossing. The data are provided by the Wind SWE [*Ogilvie et al.*, 1995] and MFI [*Lepping et al.*, 1995] experiments and are convected from the satellite to the magnetopause by about 9 min.

ionosphere are used to estimate the distance from the observing satellite to the reconnection line X_r defined by:

$$X_r/X_m = 2\ V_e/(V_m - V_e) \quad (1)$$

where X_m is the distance to the ionospheric mirror point, V_e is the cutoff velocity of the precipitating (earthward propagating) ions, and V_m is the cutoff velocity of the mirrored distribution [e.g., *Onsager et al.*, 1990; *Fuselier et al.*, 2000]. X_m is determined by using the position of the Polar spacecraft in the cusp and tracing the geomagnetic field line at this position down to the ionosphere by using the Tsyganenko 1996 (T96) model [*Tsyganenko*, 1995]. The location of the reconnection line at the magnetopause is determined by tracing the calculated distance to the reconnection site along the T96 model magnetic field lines back to the magnetopause. The method has been successfully used in several cusp studies and led to the development of the Maximum Magnetic Shear model to predict the location of the reconnection line at the dayside magnetopause [e.g., *Fuselier et al.*, 2000; *Trattner et al.*, 2007].

3. Observations

3.1. Event 1: 22 March 1996

[17] The first event discussed in this study was observed on 22 March 1996 in the Northern Hemisphere cusp by the Polar satellite. Figure 1 shows the solar wind conditions from 02:42 UT to 03:00 UT observed during this event. The data from the Wind SWE [*Ogilvie et al.*, 1995] and Wind MFI [*Lepping et al.*, 1995] experiments have been convected by about 9 min to account for the travel time between the Wind satellite and the magnetopause. The average solar wind density, N, for this cusp event was about 3 cm^{-3} (Figure 1, top) with an average solar wind velocity, V, of about 630 km/s (Figure 1, middle). Figure 1 (bottom) shows the IMF components in GSM coordinates. The IMF is dominated by the B_X component and also shows a distinctive southward direction with a brief northward field at the beginning of the Polar cusp crossing until about 02:46 UT. The IMF is relatively stable throughout the event with 3.3, 1.1, and −0.2 nT for B_X (black line), B_Y (green line), and B_Z (colored area), respectively.

[18] Figure 2 (top) shows the H^+ omnidirectional flux measurements (1/(cm^2 s sr keV/e)) as observed by the TIMAS instrument on board the Polar satellite during the 22 March 1996 cusp crossing. Polar was located in the postnoon sector around 13:00 magnetic local time (MLT) moving toward higher latitudes and encountered magnetosheath ions on open geomagnetic field lines starting at about 02:43 UT. Polar remained in the cusp until about 03:55 UT.

[19] In the vicinity of the open-closed field line boundary, the Polar cusp crossing is characterized by two major ion energy dispersions (I, II) also known as "step up cusp structures" (see Figure 2). Such cusp structures are discussed in the pulsating cusp model [e.g., *Cowley and Lockwood*, 1992; *Lockwood and Smith*, 1994] and usually interpreted as the signature of transient flux tubes on open magnetic field lines. Transient flux tubes are caused by changes in the reconnection rate at the magnetopause and convected under the joint action of magnetic tension and momentum transfer from the shocked solar wind flow. In contrast, cusp structures can also be caused by spatially separated flux tubes as a consequence of multiple reconnection lines. Such structures were also observationally confirmed in earlier studies [e.g., *Newell and Meng*, 1991; *Onsager et al.*, 1995; *Weiss et al.*, 1995; *Wing et al.*, 2001; *Trattner et al.*, 2002, 2003, 2005].

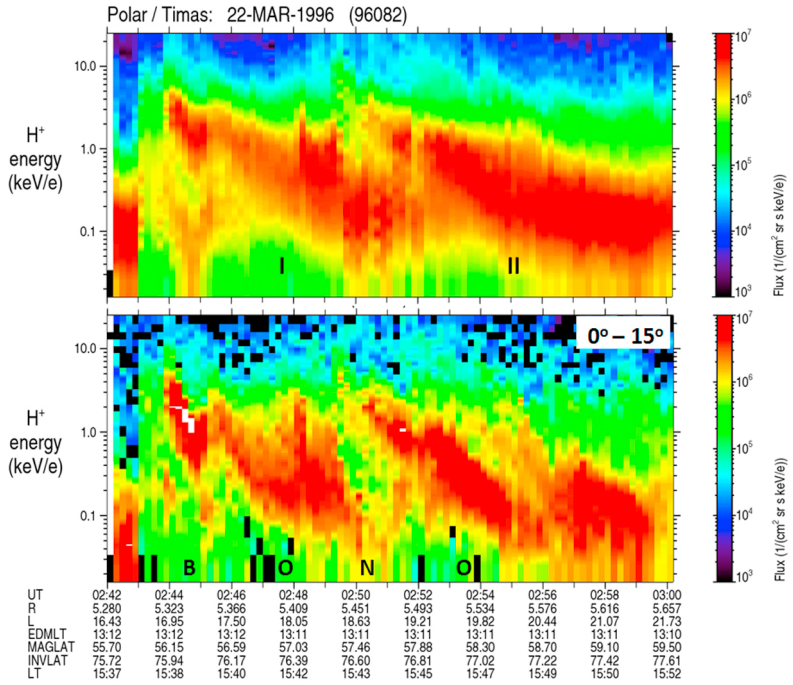

Figure 2. (top) H^+ omnidirectional flux measurements (1/(cm^2 s sr keV/e)) observed by the TIMAS instrument on board the Polar satellite during a Northern Hemisphere cusp crossing on 22 March 1996. Polar was moving toward higher latitudes and encountered magnetosheath ions on open geomagnetic field lines at about 02:43 UT. The omnidirectional flux measurements show two major cusp steps, which are partly overlapping. (bottom) H^+ flux measurements for the pitch angle range of 0°–15°, which has many more cusp structures. Although the original cusp overlap has disappeared (N), there are now two more cusp steps with clear overlaps for downward precipitating ions (O) and a boundary motion signature (B).

[20] The upward cusp structures in Figure 2 (top) show a significant overlap in energy around 02:50 UT. Such an overlap was interpreted by *Yamauchi and Lundin* [1994] as evidence for multiple access of magnetosheath plasma to the same flux tube at different times. The bottom of Figure 2 shows only the downward precipitating field-aligned ions in the pitch angle range from 0° to 15° for the Polar cusp crossing on 22 March 1996. Precipitating ions reveal that the overlap at 02:50 UT (N) disappears, supporting the interpretation by *Lockwood* [1995] that the overlap in energy occurred only for non-field-aligned ions due to their finite gyroradii. However, field-aligned precipitating ion distributions in Figure 2 also show several additional structures previously hidden in the omnidirectional flux plot. At 02:44 UT and marked by the letter B in Figure 2 (bottom), the previously decreasing ion energy dispersion slowly turns around and reaches a new energy maximum at about 02:46 UT. Such slow variations in the ion energy dispersion were previously discussed as the signature of boundary motions and changes in the convection pattern of newly opened magnetic field lines by *Trattner et al.* [2005]. Precipitating ions also reveal two true overlaps in energy (O) at 02:48 UT and 02:54 UT, which are most likely the result of reopening the already convecting flux tube, allowing for multiple access of magnetosheath plasma into the magnetosphere [e.g., *Hasegawa et al.*, 2010].

[21] Figure 3 (top) shows a two-dimensional cut through the three-dimensional H^+ distribution measured by the TIMAS instrument on Polar for the time interval from 02:45.49 UT to 02:46.01 UT on 22 March 1996. Plotted is flux in the frame where the bulk flow velocity perpendicular to the magnetic field is zero. The plane of the two-dimensional cut contains the magnetic field direction (y axis), and the orthogonal direction which lies in the plane containing the magnetic field and the Sun–Earth line (x axis). Three-dimensional flux measurements from the TIMAS instrument within ±45° of this xy plane are rotated into the plane and averaged by preserving total energy and pitch angle to produce the distribution in Figure 3 (top) [see also *Fuselier et al.*, 2000; *Trattner et al.*, 2007].

[22] Below the two-dimensional distribution is a cut through the distribution along the magnetic field direction (along the y axis of Figure 3 (top)). The solid line shows the measured flux level for this cut while the dotted line represents the one-count level. For both images in Figure 3, distributions with positive velocities are moving parallel to the geomagnetic field toward the ionosphere, while distributions with negative velocities are moving away from the ionosphere, antiparallel to the magnetospheric field.

[23] The peak of the precipitating magnetosheath distribution in Figure 3 is identified at about 410 km/s. At negative velocities, two peaks are identified, representing the mirrored magnetosheath distribution at −620 km/s and the ionospheric ion outflow distribution [e.g., *Yau et al.*, 1985; *Peterson et al.,* 2001] at approximately −220 km/s. The precipitating and mirrored ion peaks are marked with vertical solid lines (Figure 3, bottom) and horizontal dashed lines (Figure 3, top). The low-velocity cutoffs of the precipitating

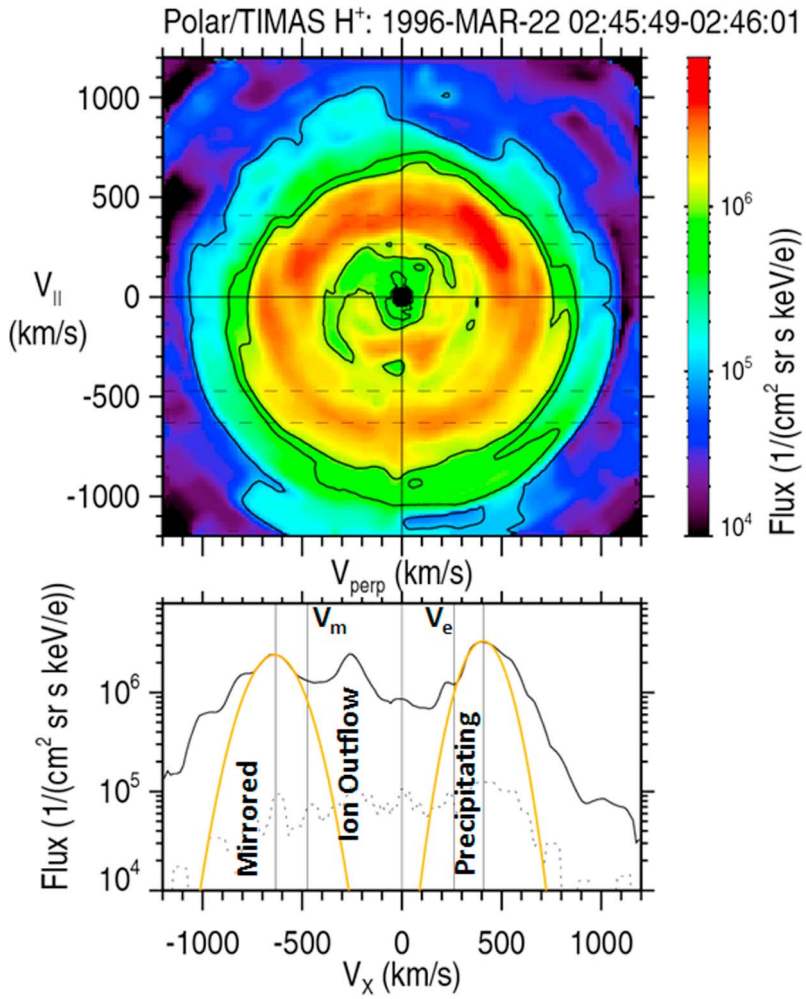

Figure 3. Two-dimensional representation of the three-dimensional H^+ ion flux distribution observed by the TIMAS instrument on board Polar during the cusp crossing on 22 March 1996. (top) The velocity space distribution in a plane containing the magnetic field direction (*y* axis) and the orthogonal direction in the plane containing the magnetic field and the Sun–Earth line (*x* axis). (bottom) The one-dimensional cut of the distribution, along the magnetic field direction. Precipitating magnetosheath ions move along the magnetic field toward the ionosphere in the Northern Hemisphere. Also indicated are the ion outflow peak common in cusp observations and the mirrored magnetosheath distribution returning from the ionosphere. The precipitating and mirrored distributions are fit with Gauss distributions (orange curves) to determine the cutoff velocities V_m and V_e used in the calculation for the distance to the reconnection site.

(V_e) and mirrored (V_m) ion distributions are defined at the low-speed side of each beam where the flux is 1/e lower than the peak flux [see also *Fuselier et al.*, 2000; *Trattner et al.*, 2005, 2007]. To ensure a clear reproducible identification of the 1/e cutoff velocity in this region, especially for the mirrored distribution close to the ionospheric outflow peak, the two-dimensional cuts of the Polar/TIMAS observations are fit with Gaussian distributions (orange curves) that are subsequently used to mark the 1/e reduced flux levels at the low-speed sides of the peak fluxes. These cutoff velocities are used in equation (1) to calculate the distance to the reconnection site. This distance is subsequently traced back to the magnetopause along T96 magnetic field lines.

[24] The result of field line traces for a series of Polar/TIMAS distribution cuts observed during the 22 March 1996 Polar cusp crossing is shown in Figure 4. The end points of the field line traces are marked with black square symbols, overlaid onto the magnetopause magnetic shear angle plot for the 22 March 1996 Polar cusp crossing. The dayside magnetopause magnetic shear angle was determined using the *Cooling et al.* [2001] analytical model as the external (magnetosheath) magnetic field and the T96 model at the *Sibeck et al.* [1991] ellipsoidal magnetopause as the internal (magnetosphere) magnetic field. Differences in the magnetopause shapes between the two models are corrected by mapping of the draped magnetosheath field conditions along the boundary normal onto the *Sibeck et al.* [1991] magnetopause.

[25] Red areas in Figure 4 represent regions where the geomagnetic fields and the draped IMF are nearly antiparallel (>150° shear angle) while blue and black areas represent regions where the merging fields become nearly

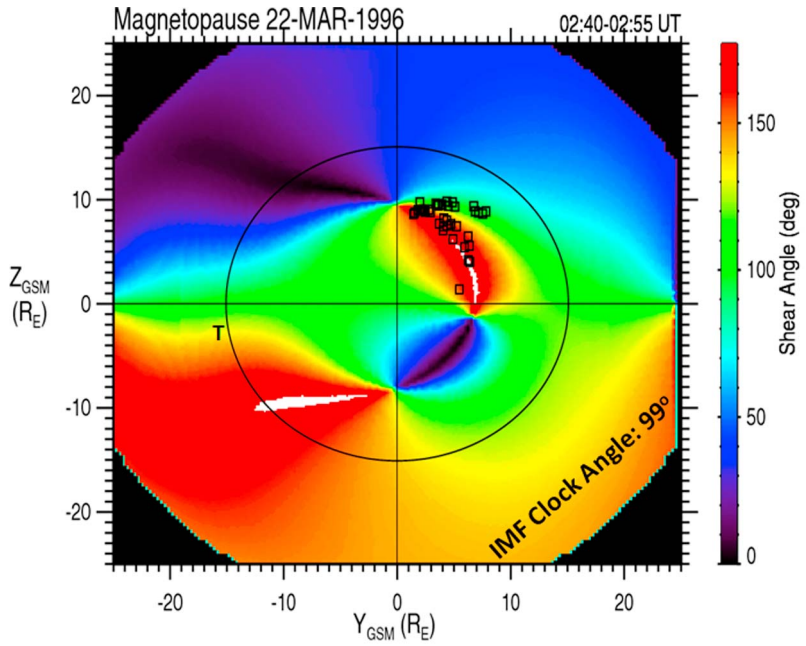

Figure 4. Magnetopause shear angle for the Polar cusp crossing on 22 March 1996, as seen from the Sun. The magnetopause shear angle was calculated using the magnetic field direction of the T96 model [*Tsyganenko*, 1995] combined with the fully draped IMF conditions at the magnetopause [*Cooling et al.* 2001] during the Polar cusp crossing. The circle represents the magnetopause shape at the terminator plane (T). The black square symbols in the region where the magnetic fields are antiparallel show the location of the reconnection site determined by the low-velocity cutoff method [e.g., *Onsager et al.*, 1990; *Trattner et al.*, 2007].

parallel. The antiparallel reconnection regions for the Polar cusp are located in the southern dawn and northern dusk region (IMF clock angle of 99°). The regions are asymmetric with respect to the hemisphere due to the dominant IMF B_X conditions. The black circle represents the location of the terminator plane (T) as it intersects the magnetopause.

[26] The field line trace points are located in the same hemisphere as the Polar satellite in the cusp, along the dusk antiparallel reconnection region, extending from the northern cusp toward the equator. The location trace points also seem to bifurcate, with another location right next to the antiparallel shear angle region at the magnetopause. However, the bifurcated points are so close together that they lie within their associated error bars (typically 1–2 R_E [see *Trattner et al.*, 2007]) and no definitive conclusion can be drawn. The separation of the reconnection site with the low-velocity method was not possible since the mirrored ion distributions for both precipitating dispersions could not be clearly identified.

[27] Figure 5 shows a series of two-dimensional cuts of the H^+ ion flux distribution from the first overlap region at 02:48 UT. The format is the same as in Figure 3. Figure 5a depicts data observed by the Polar/TIMAS instrument from 02:47.19 UT to 02:47.31 UT. The velocity of the precipitating distribution (P) from the original cusp step has decreased to about 200 km/s due to the time-of-flight effect from the reconnection site [e.g., *Rosenbauer et al.*, 1975; *Shelley et al.*, 1976; *Reiff et al.*, 1977; *Smith and Lockwood*, 1996]. The mirrored (M) and ionospheric outflow (I) distributions have almost merged into one distribution commonly seen at higher latitudes in the cusp.

[28] The second 12 s frame in Figure 5b observed from 02:47.31 UT to 02:47.43 UT shows the original precipitating distribution (P1) and a new distribution (P2) at higher energies traveling parallel to the ambient magnetic field. This overlap in energy for ions traveling parallel to the magnetic field is most likely caused by a reopening of an already open convecting flux tube at a secondary location. The reopened field line creates a magnetic island or FTE like flux rope at the magnetopause [*Lee and Fu*, 1985; *Fuselier et al.*, 1997; *Trattner et al.*, 1998; *Omidi and Sibeck*, 2007; *Hasegawa et al.*, 2010].

[29] The third 12 s time frame in Figure 5c from 02:47.43 UT to 02:47.55 UT shows a similar scenario as in the previous time frame but with the new higher energy distribution spreading out in pitch angle as slower ions arrive at the observing satellite. Such pitch angle behavior is typical for ions injected by magnetic reconnection at the magnetopause and observed in the cusp regions at some distance from the entry point.

[30] The final frame in Figure 5d shows the time interval from 02:48.31 UT to 02:48.43 UT. During that time interval the higher energy distribution has disappeared, leaving only the original distribution. This brief appearance of an additional cusp distribution is consistent with passing of a magnetic island or flux rope since only a few field lines would be affected by the secondary reconnection process at the magnetopause.

[31] Figure 6 shows 12 s flux spectra for downward precipitating protons (pitch angles 0°–15°) for the second overlap interval during the Polar cusp crossing on 22 March

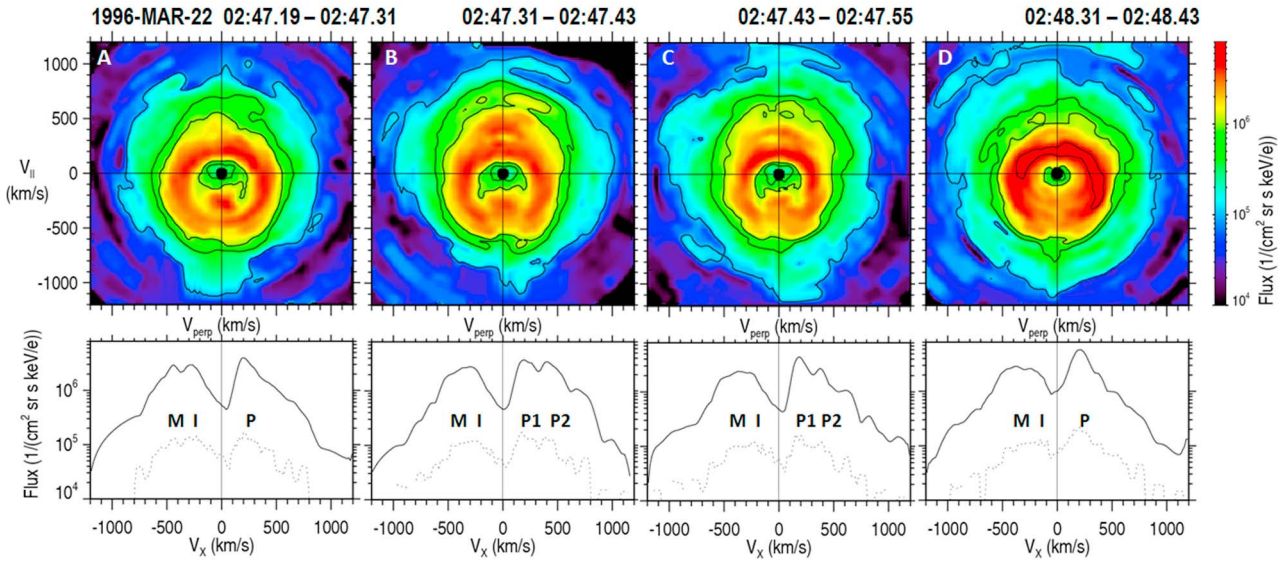

Figure 5. A series of two-dimensional cuts of the three-dimensional H^+ ion flux distribution observed by the TIMAS instrument on board Polar on 22 March 1996 during the encounter with the first cusp structure overlap (see Figure 2). The layout is the same as in Figure 3. Figure 5a shows the classical cusp plasma profile with precipitating (P), mirrored (M), and ionospheric outflow (I) distributions. A second precipitating distribution (P2) then appeared but was only present in a few subsequent frames.

1996 around 02:54 UT. The first spectrum (Figure 6, top) was observed at 02:52.30 UT and shows a precipitating distribution P3 at about 500 eV. Two minutes later at 02:54.30 UT (Figure 6, bottom), the former single distribution changed into a double distribution with peak at 200 eV (P3) and 1 keV (P4), repeating the previous cycle of forming two entry regions for this convecting flux tube.

[32] The magnetopause reconnection location for this multiple reconnection event occurred in the high-latitude Northern Hemisphere, the same hemisphere as the observing Polar satellite. There are also no sudden changes in the solar wind velocity, which rules out that variation in the particle acceleration at the magnetopause could be responsible for the overlapping cusp ion distributions [e.g., *Lockwood*, 1995]. This event appears to be more consistent with the *Lee and Fu* [1985] model. The magnetic field conditions for this event are dominated by the IMF B_X component which statistically causes high-latitude antiparallel reconnection as shown in Figure 4 and discussed in the Maximum Magnetic Shear model [*Trattner et al.*, 2007]. During dominant IMF B_X conditions, the high-latitude magnetopause is the region where the IMF makes first contact with the magnetopause, which is probably responsible for the high-latitude reconnection location and could influence the occurrence of multiple reconnection lines.

3.2. Event 2: 7 April 1996

[33] The second event discussed in this study was observed by Polar on 7 April 1996, during steady solar wind conditions with an average solar wind density of about 8 cm^{-3} and an average solar wind velocity of about 314 km/s. The IMF in GSM coordinates is also stable throughout the event with −1, 2.6, and −0.9 nT for B_X, B_Y, and B_Z, respectively. The solar wind observations by the Wind satellite are convected by 28 min to account for the travel time from the Wind satellite to the magnetopause.

[34] Figure 7 shows H^+ omnidirectional flux measurements (1/(cm^2 s sr keV/e)) for this event, observed by the TIMAS instrument on board the Polar satellite in the postnoon sector of the northern cusp. The layout of Figure 7 is the same as in Figure 2. This cusp crossing shows a bifurcation of the ion energy dispersion at the equatorward open-closed field line boundary immediately after Polar entered the cusp (O). The cusp ion dispersion starts out as a single dispersion around 05:00 UT before bifurcating. The two ion dispersions are separating in a manner similar to the prediction in the *Lockwood* [1995] model for reconnection lines located in the opposing hemisphere with respect to the observing satellite or sudden changes in the convection velocity which have not been observed for this event.

[35] Figure 8 shows the magnetopause shear angle for the Polar cusp crossing on 7 April 1996, as seen from the Sun. The layout of Figure 8 is the same as for Figure 4 with the white line representing the line of Maximum Magnetic Shear across the dayside magnetopause for the solar wind and IMF conditions during the 7 April 1996 Polar cusp crossing. The line of Maximum Magnetic Shear was documented as the most likely location for the reconnection line in a study by *Trattner et al.* [2007] based on 130 Polar cusp crossings.

[36] Black square symbols in Figure 8 represent the end points of the T96 field line trace and mark the magnetopause entry points for magnetosheath plasma observed in the cusp. The reconnection locations determined from observations with bifurcated precipitating and mirrored cusp ion distributions are also marked with blue triangles (for the original dispersion) and green diamonds (overlapping distributions). Entry points are located in the antiparallel shear angle region in the northern dusk hemisphere and not in the southern hemisphere as expected from the *Lockwood* [1995] model for

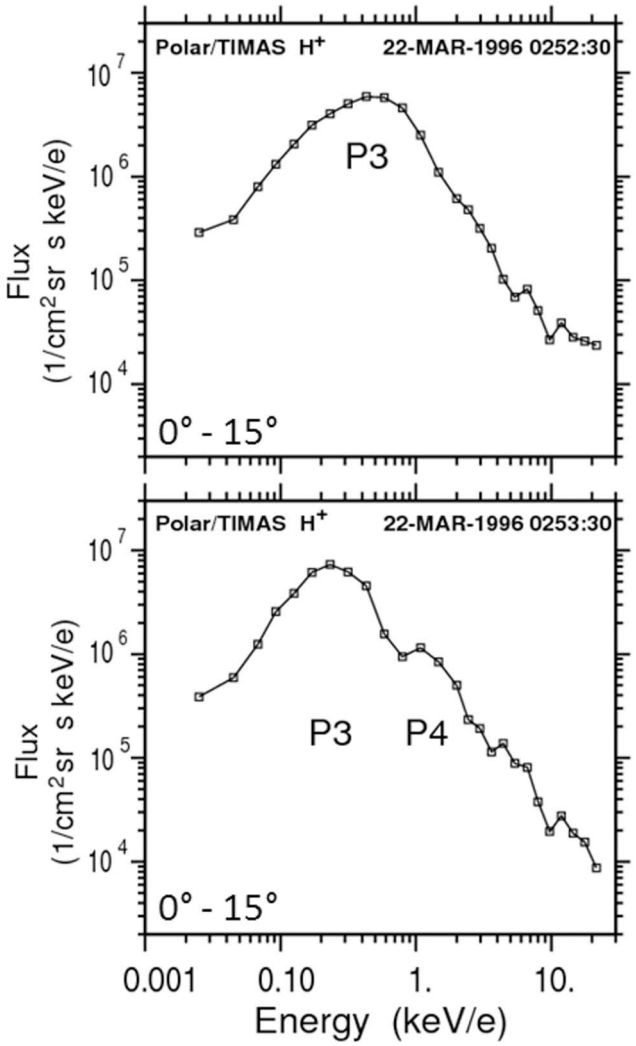

Figure 6. Two 12 s proton flux spectra in the pitch angle range from 0° to 15° observed by the TIMAS instrument on Polar for the second cusp structure during the 22 March 1996 cusp crossing. A single downward precipitating ion distribution (P3) is joined by another ion distribution (P4) at a different energy.

this type of energy bifurcation. The reconnection location also lies on the line of Maximum Magnetic Shear, which crosses the dayside magnetopause through the subsolar point and connects to the high-latitude antiparallel shear angle region at the location of the T96 field line trace points. The reconnection locations for the bifurcated dispersion events are clearly separated but within each other's error bars. The triangles and diamonds are also intermixed and located in the transition region between the antiparallel and component reconnection regions which makes a clear separation of the multiple reconnection sites difficult. This intermixture is caused when the geomagnetic field direction (used to trace the calculated distance to the reconnection site (equation (1)) to the magnetopause) is oriented along the general direction of the antiparallel reconnection region.

[37] Figure 9 shows a pair of two-dimensional cuts of the H^+ ion flux distribution for the 7 April 1996 Polar cusp crossing. The layout is the same as in Figure 3. The images depict data observed by the Polar/TIMAS instrument from 05:00.18 UT to 05:00.30 UT (Figure 9, left) and 05:00.54 UT to 05:01.06 UT (Figure 9, right). As in the previous example, there are two separate overlapping ion energy dispersions parallel to the magnetic field. In this particular event, the separation in energy increased over time (see also Figure 7, O label). An increase in the energy separation might indicate multiple reconnection locations with increasing separation relative to each other at the magnetopause (or an increase in the time since reconnection occurred for the two reconnection events).

[38] Similar to the previous event, this example shows overlapping cusp structures observed in the northern cusp which originated in the high-latitude antiparallel reconnection region in the Northern Hemisphere. With no changes in the solar wind convection speed, these overlaps are not caused by a change in ion acceleration on crossing the magnetopause. The reconnection region is located in the transition region from the antiparallel reconnection site to the tilted component reconnection line. A geomagnetic field line through that region crosses the antiparallel reconnection site as well as a component reconnection site at different locations which could help facilitate multiple reconnection events.

3.3. Event 3: 16 March 1997

[39] The third event discussed in this study was observed by Polar on 16 March 1997, during steady solar wind conditions with an average solar wind density of about 13 cm^{-3} and an average solar wind velocity of about 340 km/s. The IMF in GSM coordinates is stable throughout the period of interest with 4, −4, and −2.3 nT for B_X, B_Y, and B_Z, respectively. Observations by the Wind satellite are convected by 1 h 14 min to account for the travel time from the Wind satellite to the magnetopause.

[40] Figure 10 shows H^+ omnidirectional flux measurements (1/(cm^2 s sr keV/e)) by the TIMAS instrument for the 16 March 1997 event. The format of Figure 10 is the same as in Figure 2. The Polar spacecraft entered the northern cusp region in the postnoon sector and encountered downward precipitating magnetosheath ions at about 01:25 UT. The cusp crossing shows many cusp steps which continue until Polar crossed onto lobe field lines at about 03:20 UT. As in previous events, there are again bifurcated ion energy dispersions in the region close to the open-closed field line boundary immediately after Polar entered the cusp (O). These regions are discussed below in more detail.

[41] Figure 11 shows the magnetopause shear angle for the Polar cusp crossing on 16 March 1997, as seen from the Sun. The layout of Figure 11 is the same as for Figure 8. The black square symbols representing the location of the reconnection line from the T96 field line trace are located in the equatorial region in the component reconnection region around the predicted line of Maximum Magnetic Shear. The event also occurred close to the equinox for which the line of Maximum Magnetic Shear usually crosses the subsolar region [e.g., *Trattner et al.*, 2007] in close agreement with the traditional tilted X line component reconnection models [e.g., *Sonnerup*, 1974; *Gonzalez and Mozer*, 1974; *Cowley and Owen*, 1989, *Moore et al.*, 2002]. However, the

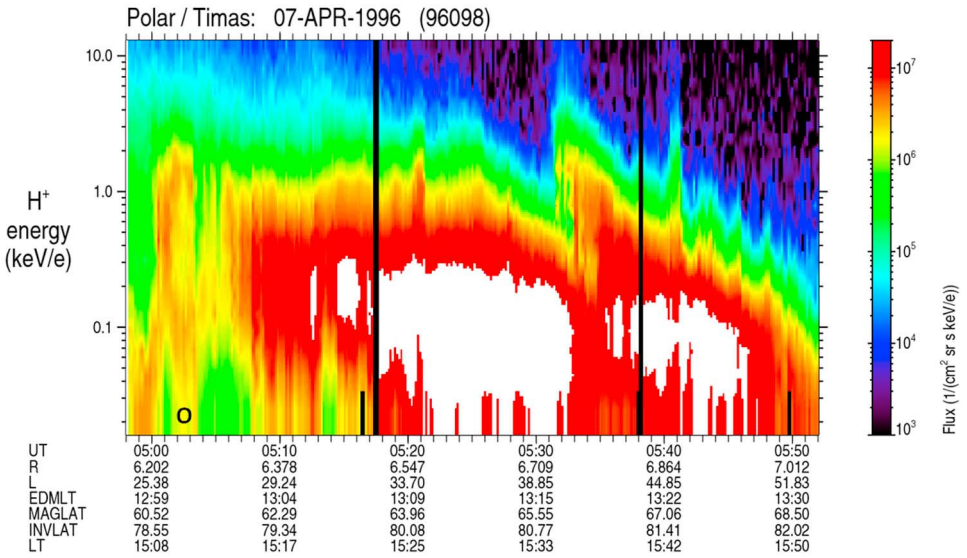

Figure 7. H^+ omnidirectional flux measurements (1/(cm^2 s sr keV/e)) observed by the TIMAS instrument on board the Polar satellite during a Northern Hemisphere cusp crossing on 7 April 1996. The layout is the same as in Figure 2. The cusp crossing shows many cusp steps and a clear bifurcation at the low-latitude edge of the cusp crossing (O).

substantial IMF B_X component during this event introduced an asymmetric magnetic shear angle distribution and moved the line of Maximum Magnetic Shear to the north. The shifted location is in agreement with the field line trace points.

[42] The trace points are also spread out over several R_E perpendicular to the line of Maximum Magnetic Shear. The trace points determined from observations with bifurcated precipitating and mirrored cusp ion distributions are also marked with blue triangles (for the original dispersion) and

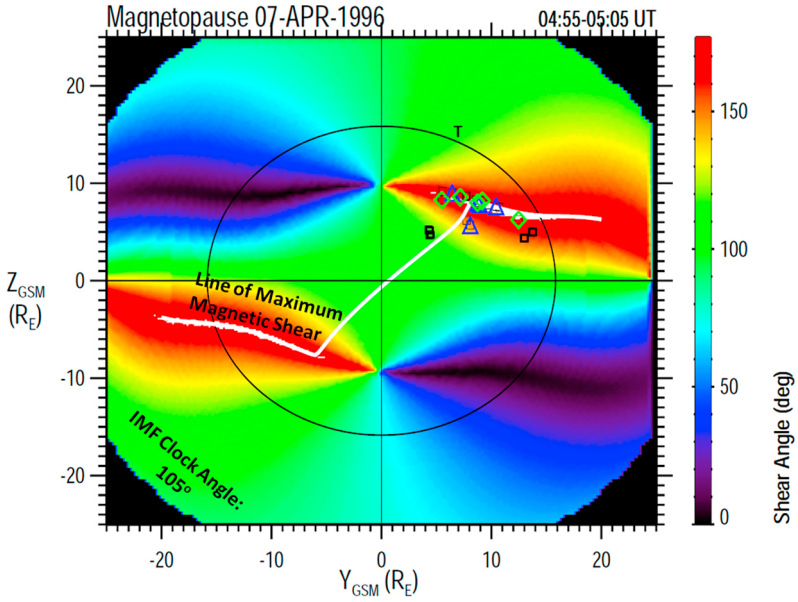

Figure 8. Magnetopause shear angle for the Polar cusp crossing on 7 April 1996, as seen from the Sun. The layout is the same as in Figure 4. The white line crossing the subsolar region shows the Line of Maximum Magnetic Shear, which depicts the most likely location of the reconnection site [see *Trattner et al.*, 2007] for the solar wind and IMF conditions observed during the cusp crossing. Black square symbols show the reconnection locations determined by the low-velocity cutoff method. For observations with overlapping cusp structures the reconnection location of the original structure is also marked by blue triangles, while the reconnection location of the overlapping structure is represented with green diamonds. The cusp field lines at the Polar satellite were opened at the antiparallel reconnection location at high latitudes.

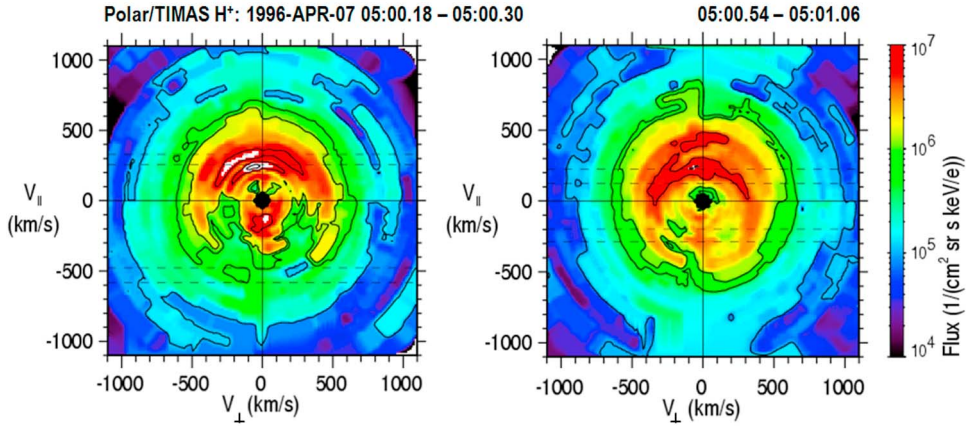

Figure 9. A series of two-dimensional cuts of the three-dimensional H^+ ion flux distribution observed by the TIMAS instrument on board Polar on 7 April 1996. The images show two downward precipitating ion distributions that are progressively separating in energy.

red diamonds (overlapping distributions). With the geomagnetic field direction nearly perpendicular to the reconnection line, the trace points for the overlapping cusp ion distributions order with respect to the line of Maximum Magnetic Shear. The trace points for the original cusp ion dispersion (blue triangles) are located south of the reconnection line while the trace points for the overlapping distribution (red diamonds) are north of the reconnection line, which depicts the formation of a magnetic island or flux rope. The distance between multiple X lines and the size of the magnetic islands is between 2 and 5 R_E.

[43] Figure 12 (top left) shows a two-dimensional cut of the H^+ ion flux distribution for the 17 March 1997 Polar cusp crossing. The layout is the same as in Figure 3. The Polar/TIMAS observation for the time frame from 01:27.57 UT to 01:28.09 UT show two clearly separated ion distributions streaming parallel to B and the associated mirrored distributions, indicating the formation of a second plasma entry point for this flux tube.

[44] Figure 12 (bottom left) shows the cut through the cusp distributions along the magnetic field direction. The peak for the precipitating magnetosheath distributions P1 and P2 are identified at about 210 km/s and 420 km/s, respectively. At negative velocities, the peaks for the mirrored magnetosheath distributions M1 and M2 are at about −320 km/s and −460 km/s, respectively. The peaks for the precipitating and mirrored ion distributions P1 and M1 are also marked with vertical solid lines (Figure 12, bottom left) and horizontal dashed lines (Figure 12, top left) and are fit with Gaussian distributions (orange curves). Also shown for P1 and M1 are the lines for the low-velocity cutoff velocities used in the calculation of the distance to the reconnection site.

[45] Figure 12 (right) shows the downward precipitating H^+ distribution in the cusp at the open-closed field line

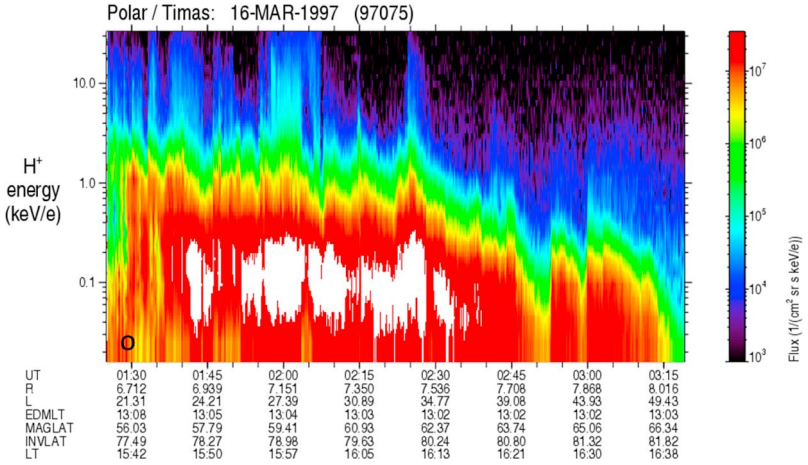

Figure 10. H^+ omnidirectional flux measurements (1/(cm^2 s sr keV/e)) observed by the TIMAS instrument on board the Polar satellite during a Northern Hemisphere cusp crossing on 16 March 1997. The layout is the same as in Figure 2. The cusp crossing is strongly structured with precipitating ions showing a brief bifurcation in energy at the low-latitude edge of the cusp crossing (O), shown in more detail in Figure 11.

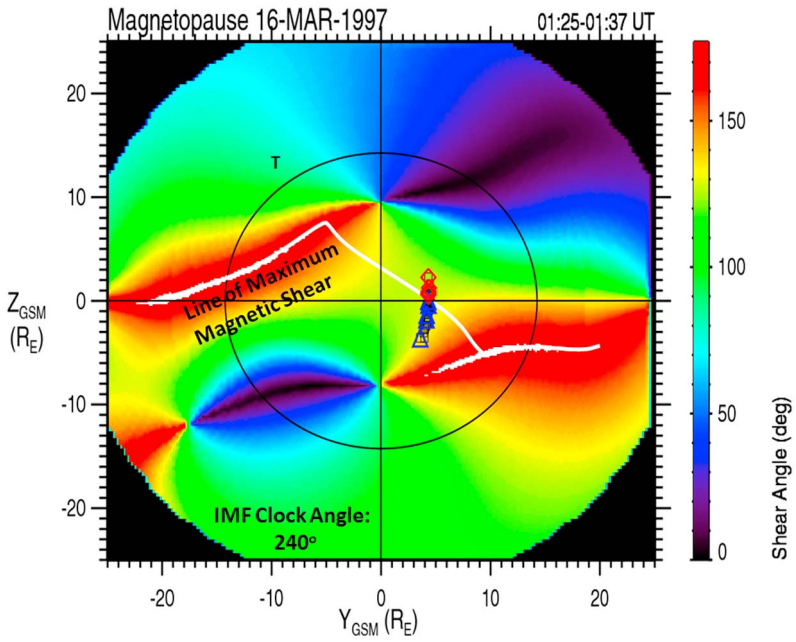

Figure 11. Magnetopause shear angle for the Polar cusp crossing on 16 March 1997, as seen from the Sun. The layout is the same as in Figure 4. The white line crossing the subsolar region shows the Line of Maximum Magnetic Shear, which depicts the most likely location of the reconnection site [see *Trattner et al.*, 2007] for the solar wind and IMF conditions observed during the cusp crossing. Black square symbols show the reconnection locations determined by the low-velocity cutoff method. For observations with overlapping cusp structures the reconnection location of the original structure is also marked by blue triangles, while the reconnection location of the overlapping structure is represented with red diamonds. The cusp field lines at the Polar satellite were opened at the component reconnection location in the equatorial region.

boundary for the 17 March 1997 Polar cusp crossing. The time interval shown in Figure 12 (left) is marked with an O. This overlap is short-lived, consistent with the passing of a magnetic island or flux tube, but followed by several additional overlaps at about 01:30 UT and 01:31 UT.

[46] As in the two previous events, this event shows no significant changes in the solar wind convection velocity that could account for the observed overlapping cusp dispersions. Magnetopause entry points for the cusp dispersions mark multiple reconnection lines located in the subsolar region around the line of Maximum Magnetic Shear. This scenario is in agreement with the *Lee and Fu* [1985] model and resembles very closely the results of the hybrid simulations by *Omidi and Sibeck* [2007].

4. Summary and Conclusions

[47] All FTE models based on time-varying reconnection at the magnetopause have support from observations at the magnetopause and in the cusp. Such widespread support raises the questions of which model represents the dominant process and what input conditions may favor one model over another. The original patchy reconnection model [*Russell and Elphic*, 1978] is supported by a statistical FTE study from the ISEE mission [*Kawano and Russell*, 2005], the bursty reconnection single X line model [*Scholer*, 1988] by AMPTE observations [e.g., *Lockwood and Hapgood*, 1998] and the multiple X lines model [e.g., *Lee and Fu*, 1985] by various studies of re-reconnection while the field line is convecting [e.g., *Fuselier et al.*, 1997; *Trattner et al.*, 1998; *Zong et al.*, 2005; *Hasegawa et al.*, 2006, 2010; *Zhang et al.*, 2008].

[48] The formation of a second entry point at the magnetopause by reopening an existing reconnected flux tube was also discussed in recent Hybrid simulations by *Omidi and Sibeck* [2007], who studied the fate of FTEs convected to the high-latitude cusp region. Multiple X lines at the dayside magnetopause are also studied in global MHD simulations by *Raeder* [2006, 2009] where multiple X lines occur preferentially for large dipole tilts, while small tilt intervals may be dominated by single X line reconnection.

[49] *Onsager* [1994] stressed that such overlapping zero pitch angle ions at different energies, observed simultaneously on convecting field lines, must have been injected at different points on the magnetopause, reopening an already open flux tube. In this study, we investigated three cusp crossings by the Polar satellite in the Northern Hemisphere which all exhibit overlapping zero pitch angle ions at different energies close to the open-closed field line boundary and favor the multiple X line model. The energy overlaps are brief, before the distributions revert back to their single ion energy dispersion typical for cusp crossings. Such brief appearances are consistent with the convection of a magnetic island or flux tube caused by re-reconnection at the magnetopause since only a few field lines enclosing the magnetic island/flux tube will undergo this process.

[50] All three events in this study were observed close to the equinox, during small dipole tilt angle times, which

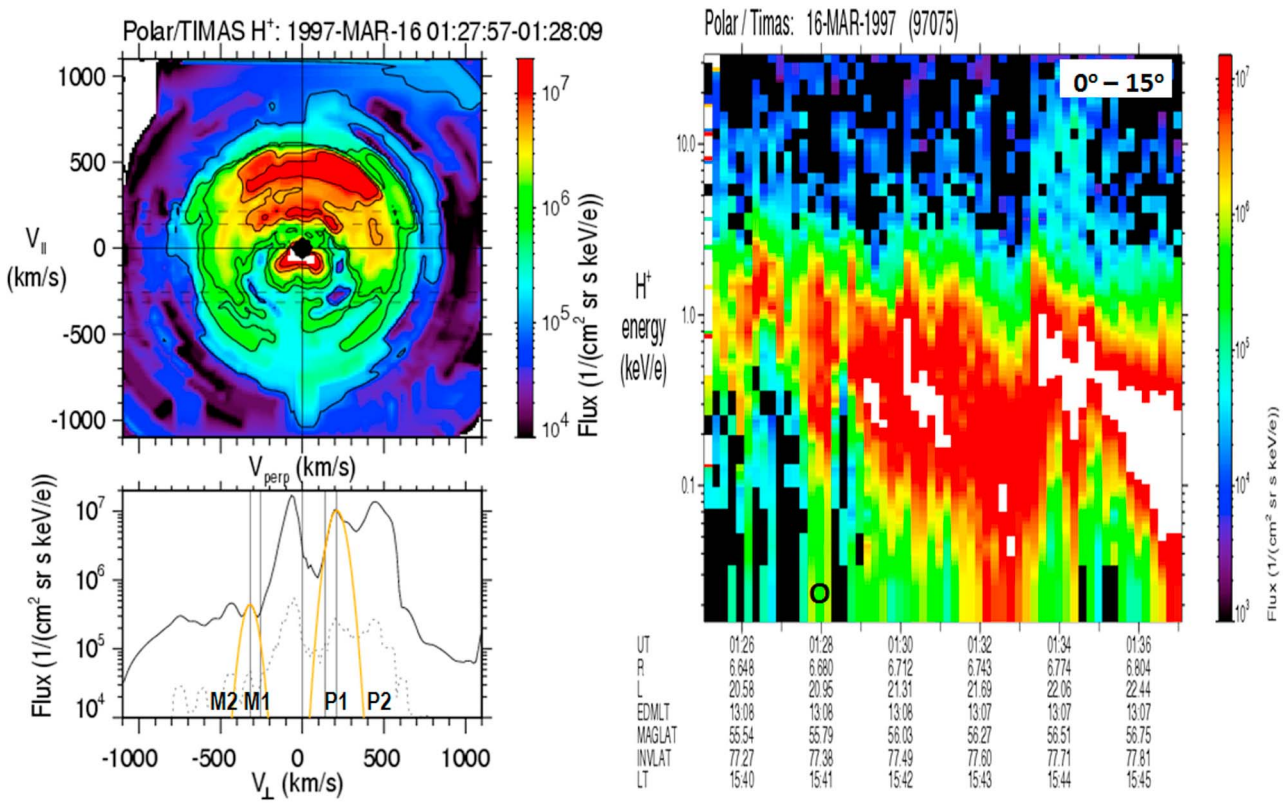

Figure 12. (left) The two-dimensional cut of the three-dimensional H^+ ion flux distribution observed by the TIMAS instrument on board Polar during the 16 March 1997 cusp crossing. The layout is the same as in Figure 3. (right) The H^+ downward precipitating ion flux (1/(cm^2 s sr keV/e)) at the equatorward edge of the cusp crossing. The time interval of the overlapping ion distribution is marked with an O.

contradicts the prediction from the MHD simulations [*Raeder*, 2006, 2009] which showed that multiple reconnection events at the dayside magnetopause mainly occur during large dipole tilt angle times. Multiple X line events in this study occurred for antiparallel reconnection (see Figure 4), in the transition region from antiparallel to component reconnection along the line of Maximum Magnetic Shear (Figure 8), and for component reconnection conditions (Figure 11) close to the magnetic equator. The formation of multiple X lines does not seem to favor specific magnetic reconnection conditions. Reconnection sites for all events are located in the same hemisphere as the observing satellite during stable solar wind and IMF conditions. Under such conditions, we do not expect sudden changes in the ion acceleration at the magnetopause for magnetosheath ions entering the magnetosphere, which is one of the possible mechanisms for generating overlapping ion pitch angle distributions in the cusp [*Lockwood*, 1995].

[51] The first and third events in this study occurred during dominant IMF B_X conditions. The influence of these specific conditions on the formation of multiple reconnection lines needs to be further investigated. Overlapping cusp ion signatures for the first two events in this paper are also discussed by *Trattner et al.* [1998]. However, analyzing techniques have significantly improved over the last decade and include now the use of the low-velocity cutoff method. This method applied to cusp distributions allows calculating the distance to the reconnection site, determining the location of the reconnection line and the local shear conditions at the reconnection site. Whenever possible this calculation was performed for both overlapping cusp dispersions. However, during the first cusp event the satellite was close to the reconnection site and the mirrored ion distribution for both dispersions could not be clearly identified. For this event the separation of the reconnection location for the two dispersions was not possible.

[52] Despite the lack of mirrored ion beams, the location trace points seem to bifurcate, though the points are so close together that they are within error bars (typically 1–2 RE [see *Trattner et al.*, 2007]) and no definitive conclusion can be drawn. Figure 4 shows trace locations covering the antiparallel reconnection site and right next to the antiparallel shear angle region at the magnetopause. For dominant IMF B_X conditions, this high-latitude antiparallel region would be the region where the IMF makes first contact with the magnetopause, which might foster a second site of reconnection on a newly opened magnetic flux tube.

[53] For the second event we were able to separate the reconnection locations for the overlapping cusp dispersions. However, the reconnection line was in the antiparallel shear angle region and was in the general direction of the geomagnetic field. These conditions caused the trace points to intermix. In Figure 8 some of the trace points continue along the antiparallel shear angle region to higher latitudes while a few trace points remain close to the line of Maximum Magnetic Shear that disconnects from the antiparallel

reconnection region at the location of the trace points and crosses the low-shear dayside magnetopause. Geomagnetic field lines in this region would cross the antiparallel shear angle region as well as the component reconnection region and reconnect first along the Maximum Magnetic Shear line and subsequently re-reconnect again at slightly higher latitudes in the antiparallel shear region.

[54] The third event is also characterized by a dominant IMF B_X component. The reconnection location is in the component reconnection region close to the subsolar point. Since the geomagnetic field lines at this location cross almost perpendicular to the predicted Maximum Magnetic Shear line, the low-velocity cutoff method was able to separate the reconnection location for the two cusp ion dispersions. While the trace points for the original cusp dispersion were traced to a place south of the reconnection line, the trace points for the overlapping dispersion were located north of the reconnection line (Figure 11). The multiple reconnection lines are separated by about 2 to 5 R_E and support the *Lee and Fu* [1985] model and are also in agreement with hybrid simulations by *Omidi and Sibeck* [2007].

[55] The Maximum Magnetic Shear line crossing the dayside magnetopause is located along a shear angle 'ridge', which often forms a flat saddle where the shear angle does not change appreciably perpendicular to the X line [e.g., *Griffiths et al.*, 2011]. The influence of the saddle on the actual location of the reconnection line still needs to be investigated further within the Maximum Magnetic Shear model; however a flat saddle might be responsible for spawning multiple X lines.

[56] The occurrence of multiple X lines shows a surprising variability with respect to magnetopause reconnection conditions. Perhaps this variability indicates why no single mechanism for FTE formation has been identified. This three event study needs to be expanded to determine if there are specific trigger mechanisms and input conditions governing the formation of multiple X lines and FTE's. Multi-spacecraft observations from, for example, Cluster could play a significant role in determining the mechanisms at work by expanding the time satellites spend in the cusp continuously and also provide a spatial component to overlapping precipitating cusp distributions.

[57] **Acknowledgments.** We acknowledge the use of the ISTP KP database. Solar wind observations were provided by the Wind Solar Wind Experiment (Wind/SWE) [*Ogilvie et al.*, 1995]. The IMF measurements were provided by the Wind Magnetic Field Instrument (Wind/MFI) [*Lepping et al.*, 1995]. The work at Lockheed Martin was supported by NASA contracts NNX08AF35G, NNX09AM72G, NNX11AJ09G, and NNG05GE15G. N. Omidi acknowledges support from NSF grant AGS-1007449.

[58] Masaki Fujimoto thanks the reviewers for their assistance in evaluating this paper.

References

Berchem, J., and C. T. Russell (1984), Flux transfer events on the magnetopause: Spatial distribution and controlling factors, *J. Geophys. Res.*, *89*, 6689–6703, doi:10.1029/JA089iA08p06689.

Boudouridis, A., H. E. Spence, and T. G. Onsager (2001), Investigation of magnetopause reconnection models using two colocated, low-altitude satellites: A unifying reconnection geometry, *J. Geophys. Res.*, *106*, 29,451–29,466, doi:10.1029/2000JA000350.

Cooling, B. M. A., C. J. Owen, and S. J. Schwartz (2001), Role of the magnetosheath flow in determining the motion of open flux tubes, *J. Geophys. Res.*, *106*, 18,763–18,775, doi:10.1029/2000JA000455.

Cowley, S. W. H., and M. Lockwood (1992), Excitation and decay of solar wind-driven flows in the magnetosphere-ionosphere system, *Ann. Geophys.*, *10*, 103–115.

Cowley, S. W. H., and C. J. Owen (1989), A simple illustrative model of open flux tube motion over the dayside magnetopause, *Planet. Space Sci.*, *37*, 1461–1475, doi:10.1016/0032-0633(89)90116-5.

Dunlop, M. W., et al. (2005), Coordinated Cluster/Double Star observations of dayside reconnection signatures, *Ann. Geophys.*, *23*, 2867–2875, doi:10.5194/angeo-23-2867-2005.

Elphic, R. C., and D. J. Southwood (1987), Simultaneous measurements of the magnetopause and flux transfer events at widely separated sites by AMPTE UKS and ISEE 1 and 2, *J. Geophys. Res.*, *92*, 13,666–13,672, doi:10.1029/JA092iA12p13666.

Farrugia, C. J., R. P. Rijnbeek, M. A. Saunders, D. J. Southwood, D. J. Rodgers, M. F. Smith, C. P. Chaloner, D. S. Hall, P. J. Christiansen, and L. J. C. Woolliscroft (1988), A multi-instrument study of flux transfer event structure, *J. Geophys. Res.*, *93*, 14,465–14,477, doi:10.1029/JA093iA12p14465.

Fuselier, S. A., et al. (1997), Bifurcated cusp ion signatures: Evidence for re-reconnection?, *Geophys. Res. Lett.*, *24*, 1471–1474, doi:10.1029/97GL01325.

Fuselier, S. A., S. M. Petrinec, and K. J. Trattner (2000), Stability of the high-latitude reconnection site for steady northward IMF, *Geophys. Res. Lett.*, *27*, 473–476, doi:10.1029/1999GL003706.

Gonzalez, W. D., and F. S. Mozer (1974), A quantitative model for the potential resulting from reconnection with an arbitrary interplanetary magnetic field, *J. Geophys. Res.*, *79*, 4186–4194, doi:10.1029/JA079i028p04186.

Griffiths, S. T., S. M. Petrinec, K. J. Trattner, S. A. Fuselier, J. L. Burch, T. D. Phan, and V. Angelopoulos (2011), A probability assessment of encountering dayside magnetopause diffusion regions, *J. Geophys. Res.*, *116*, A02214, doi:10.1029/2010JA015316.

Hasegawa, H., B. U. Ö. Sonnerup, C. J. Owen, B. Klecker, G. Paschmann, A. Balogh, and H. Reme (2006), The structure of flux transfer events recovered from Cluster data, *Ann. Geophys.*, *24*, 603–618, doi:10.5194/angeo-24-603-2006.

Hasegawa, H., et al. (2010), Evidence for a flux transfer event generated by multiple X-line reconnection at the magnetopause, *Geophys. Res. Lett.*, *37*, L16101, doi:10.1029/2010GL044219.

Kawano, H., and C. T. Russell (2005), Dual-satellite observations of the motions of flux transfer events: Statistical analysis with ISEE 1 and ISEE 2, *J. Geophys. Res.*, *110*, A07217, doi:10.1029/2004JA010821.

Le, G., C. T. Russell, and H. Kuo (1993), Flux transfer events: Spontaneous or driven?, *Geophys. Res. Lett.*, *20*, 791–794, doi:10.1029/93GL00850.

Le, G., J. T. Gosling, C. T. Russell, R. C. Elphic, M. F. Thomsen, and J. A. Newbury (1999), The magnetic and plasma structure of flux transfer events, *J. Geophys. Res.*, *104*, 233–245, doi:10.1029/1998JA900023.

Lee, L. C., and Z. F. Fu (1985), A theory of magnetic flux transfer at the Earth's magnetopause, *Geophys. Res. Lett.*, *12*, 105–108, doi:10.1029/GL012i002p00105.

Lepping, R. P., et al. (1995), The WIND magnetic field instrument, *Space Sci. Rev.*, *71*, 207–229, doi:10.1007/BF00751330.

Lockwood, M. (1995), Overlapping cusp ion injections: An explanation invoking magnetopause reconnection, *Geophys. Res. Lett.*, *22*, 1141–1144, doi:10.1029/95GL00811.

Lockwood, M., and M. Hapgood (1998), On the cause of a magnetospheric flux transfer event, *J. Geophys. Res.*, *103*, 26,453–26,478, doi:10.1029/98JA02244.

Lockwood, M., and M. F. Smith (1994), Low and middle altitude cusp particle signatures for general magnetopause reconnection rate variations: 1. Theory, *J. Geophys. Res.*, *99*, 8531–8553, doi:10.1029/93JA03399.

Lockwood, M., and J. A. Wild (1993), On the quasi-periodic nature of magnetopause flux transfer events, *J. Geophys. Res.*, *98*, 5935–5940, doi:10.1029/92JA02375.

Lockwood, M., et al. (2001), Coordinated Cluster and ground-based instrument observations of transient changes in the magnetopause boundary layer during an interval of predominantly northward IMF: Relation to reconnection pulses and FTE signatures, *Ann. Geophys.*, *19*, 1613–1640, doi:10.5194/angeo-19-1613-2001.

Moore, T. E., M.-C. Fok, and M. O. Chandler (2002), The dayside reconnection X line, *J. Geophys. Res.*, *107*(A10), 1332, doi:10.1029/2002JA009381.

Newell, P. T., and C.-I. Meng (1991), Ion acceleration at the equatorward edge of the cusp: Low altitude observations of patchy merging, *Geophys. Res. Lett.*, *18*, 1829–1832, doi:10.1029/91GL02088.

Ogilvie, K. W., et al. (1995), SWE: A comprehensive plasma instrument for the WIND spacecraft, *Space Sci. Rev.*, *71*, 55–77, doi:10.1007/BF00751326.

Omidi, N., and D. G. Sibeck (2007), Flux transfer events in the cusp, *Geophys. Res. Lett.*, *34*, L04106, doi:10.1029/2006GL028698.

Onsager, T. G. (1994), A quantitative model of magnetosheath plasma in the low-latitude boundary layer, cusp, and mantle, in *Physical Signatures of Magnetospheric Boundary Layer Processes*, *NATO ASI Ser.,Ser. C*, vol. 425, edited by J. A. Holtet and A. Egeland, pp. 385–400, Kluwer Acad., Dordrecht, Netherlands.

Onsager, T. G., M. F. Thomsen, J. T. Gosling, and S. J. Bame (1990), Electron distributions in the plasma sheet boundary layer: Time-of-flight effects, *Geophys. Res. Lett.*, *17*, 1837–1840, doi:10.1029/GL017i011p01837.

Onsager, T. G., M. F. Thomsen, R. C. Elphic, and J. T. Gosling (1991), Model of electron and ion distributions in the plasma sheet boundary layer, *J. Geophys. Res.*, *96*, 20,999–21,011, doi:10.1029/91JA01983.

Onsager, T. G., S.-W. Chang, J. D. Perez, J. B. Austin, and L. X. Jano (1995), Low-altitude observations and modeling of quasi-steady magnetopause reconnection, *J. Geophys. Res.*, *100*, 11,831–11,843, doi:10.1029/94JA02702.

Peterson, W. K., H. L. Collin, A. W. Yau, and O. W. Lennartsson (2001), Polar/Torodial Imaging Mass-Angle Spectrograph observations of suprathermal ion outflow during solar minimum conditions, *J. Geophys. Res.*, *106*, 6059–6066, doi:10.1029/2000JA003006.

Raeder, J. (2006), Flux transfer events: 1. Generation mechanism for strong southward IMF, *Ann. Geophys.*, *24*, 381–392, doi:10.5194/angeo-24-381-2006.

Raeder, J. (2009), FTE generation for predominantly east–west IMF, *Eos Trans. AGU*, *90*(52), Fall Meet. Suppl., Abstract SM31A-1516.

Reiff, P. H., T. W. Hill, and J. L. Burch (1977), Solar wind plasma injections at the dayside magnetospheric cusp, *J. Geophys. Res.*, *82*, 479–491, doi:10.1029/JA082i004p00479.

Rijnbeek, R. P., S. W. H. Cowley, D. J. Southwood, and C. T. Russell (1984), A survey of dayside flux transfer events observed by ISEE 1 and 2 magnetometers, *J. Geophys. Res.*, *89*, 786–800, doi:10.1029/JA089iA02p00786.

Rosenbauer, H., H. Grünwaldt, M. D. Montgomery, G. Paschmann, and N. Sckopke (1975), Heos 2 plasma observations in the distant polar magnetosphere: The plasma mantle, *J. Geophys. Res.*, *80*, 2723–2737, doi:10.1029/JA080i019p02723.

Russell, C. T., and R. C. Elphic (1978), Initial ISEE magnetometer results: Magnetopause observations, *Space Sci. Rev.*, *22*, 681–715, doi:10.1007/BF00212619.

Russell, C. T., and R. C. Elphic (1979), ISEE observations of flux transfer events at the dayside magnetopause, *Geophys. Res. Lett.*, *6*, 33–36, doi:10.1029/GL006i001p00033.

Russell, C. T., G. Le, and H. Kuo (1996), The occurrence rate of flux transfer events, *Adv. Space Res.*, *18*, 197–205, doi:10.1016/0273-1177(95)00965-5.

Scholer, M. (1988), Magnetic flux transfer at the magnetopause based on single X line bursty reconnection, *Geophys. Res. Lett.*, *15*, 291–294, doi:10.1029/GL015i004p00291.

Shelley, E. G., R. D. Sharp, and R. G. Johnson (1976), He^{++} and H^{+} flux measurements in the day side cusp: Estimates of convection electric field, *J. Geophys. Res.*, *81*, 2363–2370, doi:10.1029/JA081i013p02363.

Shelley, E. G., et al. (1995), The Toroidal Imaging Mass-Angle Spectrograph (TIMAS) for the Polar mission, *Space Sci. Rev.*, *71*, 497–530, doi:10.1007/BF00751339.

Sibeck, D. G., R. E. Lopez, and E. C. Roelof (1991), Solar wind control of the magnetopause shape, location, and motion, *J. Geophys. Res.*, *96*, 5489–5495, doi:10.1029/90JA02464.

Smith, M. F., and M. Lockwood (1996), Earth's magnetospheric cusp, *Rev. Geophys.*, *34*, 233–260, doi:10.1029/96RG00893.

Sonnerup, B. U. Ö. (1974), Magnetopause reconnection rate, *J. Geophys. Res.*, *79*, 1546–1549, doi:10.1029/JA079i010p01546.

Trattner, K. J., A. J. Coates, A. N. Fazakerley, A. D. Johnstone, H. Balsiger, J. L. Burch, S. A. Fuselier, W. K. Peterson, H. Rosenbauer, and E. G. Shelley (1998), Overlapping ion populations in the cusp: Polar/TIMAS results, *Geophys. Res. Lett.*, *25*, 1621–1624, doi:10.1029/98GL01060.

Trattner, K. J., S. A. Fuselier, W. K. Peterson, and C. W. Carlson (2002), Spatial features observed in the cusp under steady solar wind conditions, *J. Geophys. Res.*, *107*(A10), 1288, doi:10.1029/2001JA000262.

Trattner, K. J., et al. (2003), Cusp structures: Combining multi-spacecraft observations with ground based observations, *Ann. Geophys.*, *21*, 2031–2041, doi:10.5194/angeo-21-2031-2003.

Trattner, K. J., S. A. Fuselier, S. M. Petrinec, T. K. Yeoman, C. Mouikis, H. Kucharek, and H. Reme (2005), The reconnection sites of spatial cusp structures, *J. Geophys. Res.*, *110*, A04207, doi:10.1029/2004JA010722.

Trattner, K. J., J. S. Mulcock, S. M. Petrinec, and S. A. Fuselier (2007), Probing the boundary between antiparallel and component reconnection during southward interplanetary magnetic field conditions, *J. Geophys. Res.*, *112*, A08210, doi:10.1029/2007JA012270.

Tsyganenko, N. A. (1995), Modeling the Earth's magnetospheric magnetic field confined within a realistic magnetopause, *J. Geophys. Res.*, *100*, 5599–5612, doi:10.1029/94JA03193.

Weiss, L. A., P. H. Reiff, H. C. Carlson, E. J. Weber, and M. Lockwood (1995), Flow-alignment jets in the magnetospheric cusp: Results from the Geospace Environment Modeling Pilot program, *J. Geophys. Res.*, *100*, 7649–7659, doi:10.1029/94JA03360.

Wild, J. A., et al. (2001), First simultaneous observations of flux transfer events at the high-latitude magnetopause by the Cluster spacecraft and pulsed radar signatures in the conjugate ionosphere by the CUTLASS and EISCAT radars, *Ann. Geophys.*, *19*, 1491–1508, doi:10.5194/angeo-19-1491-2001.

Wild, J. A., et al. (2005), Simultaneous in-situ observations of the signatures of dayside reconnection at the high- and low-latitude magnetopause, *Ann. Geophys.*, *23*, 445–460, doi:10.5194/angeo-23-445-2005.

Wing, S., P. T. Newell, and J. M. Rouhoniemi (2001), Double cusp: Model prediction and observational verification, *J. Geophys. Res.*, *106*, 25,571–25,593, doi:10.1029/2000JA000402.

Yamauchi, M., and R. Lundin (1994), Classification of large-scale and meso-scale ion dispersion patterns observed by Viking over the cusp-mantle region, in *Physical Signatures of Magnetospheric Boundary Layer Process*, *NATO ASI Ser., Ser. C.*, vol. 425, edited by J. A. Holtet and A. Egeland, pp. 99–109, Kluwer Acad., Dordrecht, Netherlands.

Yau, A. W., E. G. Shelley, W. K. Peterson, and L. Lenchyshyn (1985), Energetic auroral and polar ion outflow at DE 1 altitudes: Magnitude, composition, magnetic activity dependence and long-term variations, *J. Geophys. Res.*, *90*, 8417–8432, doi:10.1029/JA090iA09p08417.

Zhang, H., K. K. Khurana, M. G. Kivelson, V. Angelopoulos, Z. Y. Pu, Q.-G. Zong, J. Liu, and X.-Z. Zhou (2008), Modeling a force-free flux transfer event probed by multiple Time History of Events and Macroscale Interactions during Substorms (THEMIS) spacecraft, *J. Geophys. Res.*, *113*, A00C05, doi:10.1029/2008JA013451.

Zong, Q.-G., et al. (2005), Plasmoid in the high latitude boundary/cusp region observed by Cluster, *Geophys. Res. Lett.*, *32*, L01101, doi:10.1029/2004GL020960.

S. A. Fuselier, S. M. Petrinec, and K. J. Trattner, Advanced Technology Center, Lockheed Martin Space Systems Company, 3251 Hanover St., Bldg. B255, A022S, Palo Alto, CA 94304, USA. (karlheinz.j.trattner.dr@lmco.com)

N. Omidi, Solana Scientific Inc., 777 Pacific Coast Hwy., Ste. 208B, Solana Beach, CA 92075, USA.

D. G. Sibeck, NASA Goddard Space Flight Center, 8800 Greenbelt Rd., NASA/GSFC Mail Code 674, Greenbelt, MD 20771, USA.